Fikry et al. Mechanics of Advanced Materials and Modern Processes (2018) 4:3
https://doi.org/10.1186/s40759-018-0036-6

Mechanics of Advanced Materials and Modern Processes

RESEARCH Open Access

The effect of matrix cracking on mechanical properties in FRP laminates

M.J. Mohammad Fikry[1*], Shinji Ogihara[2] and Vladimir Vinogradov[3]

Abstract

Background: Fiber Reinforced Polymer (FRP) laminates have properties, which are highly dependent on the ply fiber orientations and which can be designed for optimum laminate performance. The purpose of this study is to investigate the effect of matrix cracking on the mechanical properties of FRP laminates with various off-axis angles, and to provide a critical test for an analytical solution using variational stress analysis.

Methods: Carbon and glass fiber reinforced polymer laminates (CFRP and GFRP) are tested. FRP prepregs are cured by using autoclave method to form laminates with layups $[\theta_m/\ \varphi_n]_s$. The laminates are then loaded monotonically and cyclically to obtain their mechanical properties and the effect of matrix cracks on the properties. Some of the effects include reduction of laminates' stiffness and residual strains after unloading. In order to obtain higher crack densities in specimens, artificial cracks method was introduced in this study, where notches were made at the edges of some specimens before tested in tension. Cracks observation for CFRP laminates is done by using the X-ray technique, while for GFRP laminates a DSLR camera is used.

Results: The measured stiffness reduction as a function of the crack density is compared to an analytical prediction for cracked angle-ply laminates based on a variational stress analysis. The experimental results for stiffness reduction agree well with the analytical results.

Conclusion: Understanding the behavior of damaged laminates with simple configurations, as performed in this study, is of high importance for prediction of damage effects on laminates with more complex configuration, e.g. with quasi-isotropic layups.

Keywords: Composites laminate, Matrix cracking, Stiffness reduction, Artificial cracks, Crack density, Damage behavior

Introduction

Fiber Reinforced Plastics (FRP) are used in many industries, such as aeronautical, automotive, construction and etc. While many designs, especially in aeronautical applications, aim at composite structures made of quasi-isotropic material, various stacking sequences can be designed for a specific composite structural element by modifying the distribution of ply orientations through the laminate thickness. With different combinations of fiber orientations, ply thicknesses and stacking sequences that can by suggested by the designers; understanding and characterization of damage formation and its effects on the laminate effective properties can be quite complicated. Understanding the basic damage behavior and changes in the laminates with various off-axis plies due to damage, can be a step in understanding laminates with more complex configuration.

Many damage modes can be observed in laminates, such as transverse cracking, delamination, fiber fracture, longitudinal splitting and etc. Usually during tensile loading, laminates would initially demonstrate formation of matrix intralaminar cracks in the most off-axis plies (Jones 1975). The formed cracks can have significant influence on the local stress redistribution as well as the effective stiffness of the laminate. These cracks lead to reduction of the laminate stiffness, residual strains after unloading, and other phenomena.

* Correspondence: writetofikry@yahoo.com
[1]Department of Mechanical Engineering, Graduate School of Science and Technology, Tokyo, University of Science, 2641 Yamazaki, Noda-shi, Chiba-ken, Japan
Full list of author information is available at the end of the article

Table 1 Type of materials

	CFRP[1]	CFRP[2]	GFRP
	T700SC/2500, Torayca	T700SC/2592, Torayca	GE352G135SB, Mitsubishi Rayon
Ply thickness	0.05 mm	0.15 mm	0.101 mm
Type	Prepreg (preimpregnated composite fiber)		

Modeling of stiffness reduction due to matrix damage has been the topic of extensive research in the recent decades, especially for cross-ply laminates (e.g., Nairn 1992; Nairn & Shoefeng 1992; Tong & et al. 1997). The variational approach, employed in this study, was originated by Hashin (1988, 1985), who has constructed an admissible stress field, which satisfies equilibrium and all boundaries and interface condition and determined stiffness reduction and stresses on the basis of the principle of minimum complementary energy for cross-ply laminates. The analysis leads to the lower bound for the effective stiffness of cracked cross-ply laminates, which is found in agreement with some experimental data. Vinogradov and Hashin (2010) extended the analysis to angle-ply laminates of type $[\theta_m/\phi_n]_s$ containing intralaminar cracks in the middle laminae and found that prediction for the Young's modulus of cracked GFRP angle-ply $[0/45]_s$ is in good agreement with experimental results of Katerelos et al. (2006). In the recent years the variational approach has gained significant attention (e.g., Li and Hafeez 2009; Katerelos et al. 2015).

Many other methods have also been suggested. For example, Singh (2008) presented a synergistic methodology to analyze damage behavior in composite laminates with transverse matrix cracks in plies of multiple orientations. The approach combines the strengths of micro-damage mechanics (MDM) and continuum damage mechanics (CDM) in predicting the stiffness degradation due to the presence of transverse cracks.

Various experimental studies have been also conducted to characterize the effects of intralaminar damage on the mechanical properties of laminates, with less attention to laminates with middle laminae at angles other than 90°. For example, Highsmith and Reifsnider (1982), experimentally studied the degradation of the mechanical response of composite materials, as determined via stiffness measurements resulting from transverse cracking. In this study, observation on the damage development in quasi-isotropic ($[0/\pm45/90]_s$ and $[0/90/\pm45]_s$) carbon–epoxy laminates under fatigue loading was conducted.

Nouri et al. (2013) investigates the effect of pre-existing diffuse damage on the evolution of transverse cracking in cross-ply CFRP laminates; they found that diffuse damage has a great effect on the transverse cracking process. Transverse cracking is defined as meso-scale cracks propagating throughout the whole thickness of the elementary ply. In the case of transverse loading, these cracks initiate early on and are the predominant form of damage. They appear much later in shear loading after multiple debonded surfaces have merged together. It is well known that this mechanism is dependent on the ply thickness.

Most of the studies were focused only on glass epoxy material and also the laminates with off-axis plies of 90°. (e.g., Bassam et al. 1998; Harrison & Bader 1983). In this paper, we study damage formation and its effect on the mechanical properties of FRP laminates with various stacking sequences $[\theta_m/\phi_n]_s$ prepared from two different CFRP prepregs and one GFRP prepreg materials. The materials are; CFRP Torayca (T700SC/2500) - applied in general purpose/industry such as sporting equipment and etc., CFRP Torayca (T700SC/2592) - used also in general purpose but with heat-resistant tough resin, and lastly GFRP Mitsubishi Rayon (GE352G135SB).

The laminate configurations used in this study may not be of great real-life practical layups, but their stiffness reduction due to matrix cracking are large enough to provide a critical test for an analytical prediction and also to allow a check for stacking sequence dependence.

Methods/experimental

Specimen

The materials used in this study and the properties of unidirectional materials are shown in Tables 1 and 2 respectively.

Table 2 Unidirectional material properties

	CFRP[1] (T700SC/2500)	CFRP[2] (T700SC/2592)	GFRP (GE352G135SB)
Young's modulus in 0° direction E_1 [GPa]	130	123	38.2
Young's modulus in 90° direction E_2 [GPa]	9.53	8.68	11.1
Shear modulus G_{12} [GPa]	3.18	3.92	3.94
Poisson's ratio v_{12} [–]	0.34	0.33	0.31

Table 3 Laminate structures and thicknesses

Materials	Laminate structures	Thickness (mm)
CFRP [1] (T700SC/2500)	$[0_3/90_{24}/0_3]$, $[0_3/75_{24}/0_3]$, $[0_3/45_{24}/0_3]$	1.50
	$[0_3/90_{36}/0_3]$, $[0_3/75_{36}/0_3]$, $[0_3/45_{36}/0_3]$	2.10
CFRP [2] (T700SC/2592)	$[0/90_8/0]$, $[0/60_8/0]$, $[0/45_8/0]$	1.47
	$[0/90_{12}/0]$, $[0/60_{12}/0]$, $[0/45_{12}/0]$	2.06
GFRP (GE352G135SB)	$[0_3/90_{12}/0_3]$	1.80
	$[0_3/90_{24}/0_3]$, $[0_3/75_{24}/0_3]$	3.00
	$[-15_3/75_{24}/-15_3]$, $[0_3/60_{24}/0_3]$	3.00

The prepregs are stacked according to the stacking sequences shown in Table 3 and cured in an autoclave at a temperature of 130 °C and pressure of 0.2 MPa. The specimen's measurements are shown in Fig. 1. Laminates are cut into the measurement by using a composite material cutting machine (AC-300CF, Maruto Testing Machine). The ends of both the laminates and GFRP tabs are polished by using sandpaper (#1200) to improve adhesion when glued. GFRP tabs are glued to the specimen ends by using adhesive glue (Araldite-Standard, Huntsman Japan) before the tensile testing.

For each material the prepreg thickness is different, the number of plies used were also different in order to

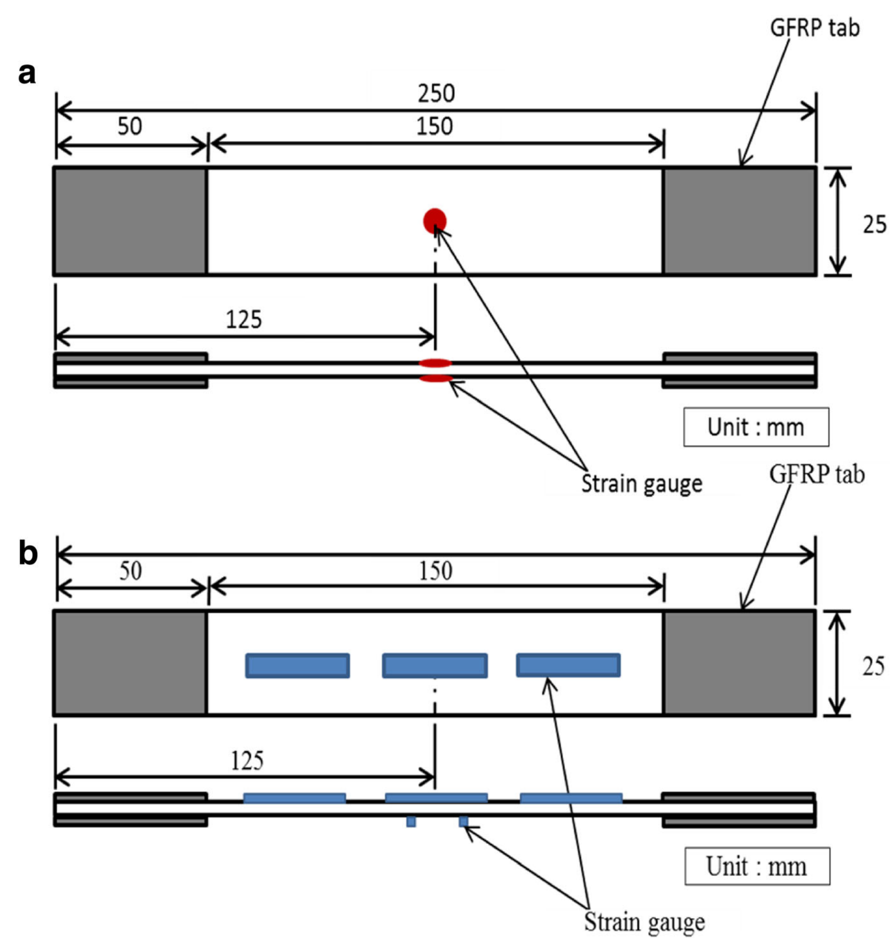

Fig. 1 Specimen's measurement **a** monotonic tensile test **b** loading-unloading tensile test

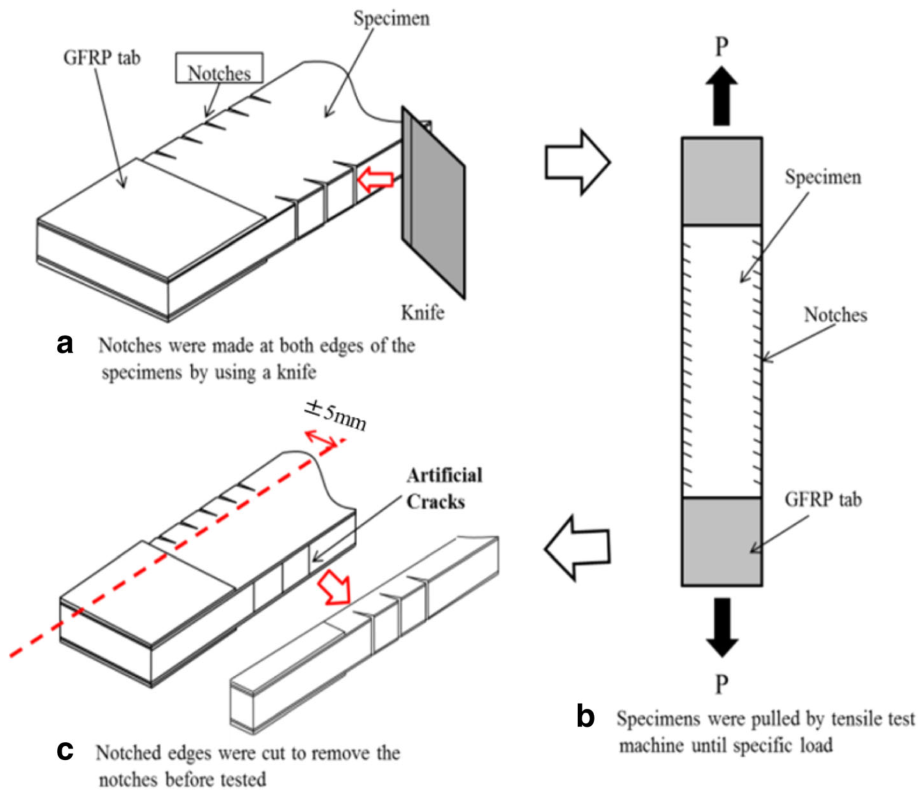

Fig. 2 Method used to induce artificial cracks. **a** Notches at the edges of the specimen, **b** Loading of notched specimen to induce artificial cracks, **c** Notches were remove after loaded

produce laminates with about the same thickness. This is to compare the mechanical properties and the effects of matrix cracking in the materials.

Artificial cracks

In contrast to laminate with off-axis angle of 90°, crack formation in laminate with different off-axis angles require significantly higher tensile loads due to the higher material stiffness. In order to increase the range of attained cracks densities for the purpose of validation of the variational analysis (Vinogradov, 2015), artificial crack method is introduced in this study (Fig. 2) when notches are formed at both edges of the specimen by using a knife before it is pulled in a tensile test machine with cross head speed of 1 mm/min to a specific load. Then the specimen is unloaded back to zero and the notched edges were cut by using composite material cutting machine (AC-300CF, Maruto Testing Machine) at ±5 mm from the edges. To detect the artificial cracks induced, observation in an X-ray machine was carried out before it was tested in tension.

Tensile tests and measurement

Two types of experiments were carried out using Tensilon RTF-1350 A & D tensile test machine: monotonic and loading-unloading tensile tests. Both of the experiments were performed with the cross head displacement speed of 1 mm/min.

The mechanical properties obtained from monotonic tensile test are tensile stress, longitudinal strain, transverse strain, the Young's modulus and Poisson's ratio. The loading-unloading tests were performed to investigate the mechanical properties affected by crack formation. For CFRP laminates, as the laminates are

Table 4 Strain gauges used in experiments

Monotonic tensile test	Biaxial 0°/90° stacked rosette strain gauge (KFGS-2-120-D16–11L1M2S)
Loading-unloading tensile test	Uniaxial strain gauge stacked in loading direction (KFGS-30-120-C1-11L3M2R) Uniaxial strain gauge stacked in perpendicular to loading direction (KFGS-5-120-C1-11L1M2R)

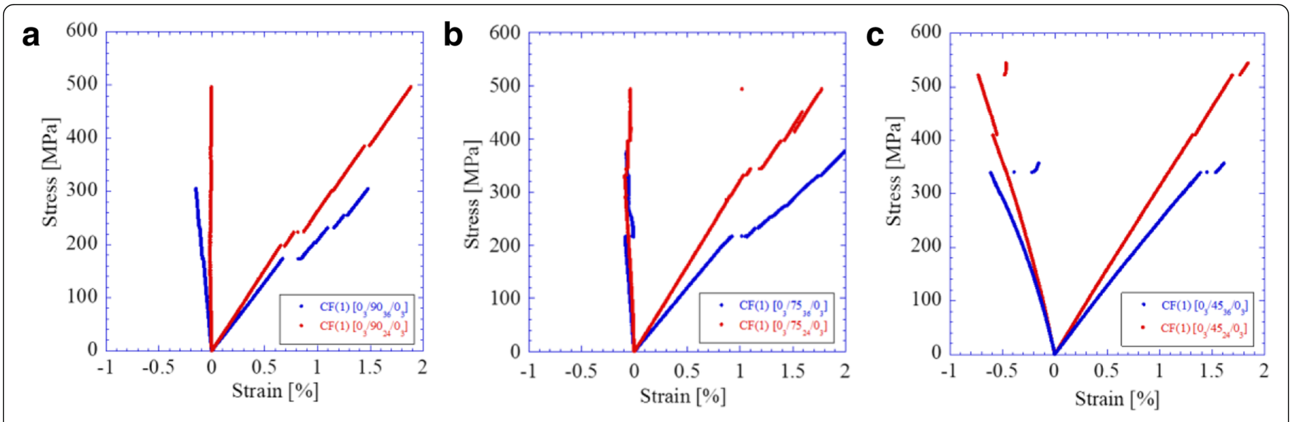

Fig. 3 Strain-stress curve for CFRP[1] laminates with different orientation of the off-axis ply: **a** 90, **b** 75 and **c** 45°

opaque, crack observations was done using X-ray; while for semi-transparent GFRP laminates, cracks were observed in-situ using a DSLR camera. Strain gauges were used to measure strains in the loaded and unloaded laminates, see Table 4. For more accurate strain readings, three uniaxial strain gauges were stacked in the loading direction (Fig. 2b). In this study, the crack density is defined as the number of cracks penetrated in the width direction over the length of strain gauges.

Results and discussion

Monotonic tensile test

Strain gauges were attached in both the longitudinal and transverse directions for strain measurements in both the directions. The Young's modulus of every laminates was calculated at small strains of 0.1~ 0.3% when no cracks are typically formed. Nonlinearity of the stress-strain curves is correlated with the formation of cracks.

CFRP laminates

Figure 3 shows the stress-strain curves for CFRP [1] specimens: (a) $[0_3/90_{24}/0_3]$ and $[0_3/90_{36}/0_3]$, (b) $[0_3/75_{24}/0_3]$ and $[0_3/75_{36}/0_3]$, and (c) $[0_3/45_{24}/0_3]$ and $[0_3/45_{36}/0_3]$ laminates. Figure 4 shows the stress-strain curve for CFRP[2] specimens: (a) $[0/90_8/0]$ and $[0/90_{12}/0]$, (b) $[0/60_8/0_3]$ and $[0/60_{12}/0]$, and (c) $[0/45_8/0]$ and $[0/45_{12}/0]$ laminates. Table 5 summarizes the mechanical properties (obtained from the average of three laminate specimens of the same layup) of the CFRP laminates tested. During the tensile test to obtain these stress-strain curve, 2 mm strain gauges were pasted at the center of the specimen at both sides. When cracks occur on the area where strain gauges were pasted, this caused a sudden increase or jump of strain value. This is the reason why it can be observed that the stress-strain curves were not continuing and have some skipped zones.

Comparison of CFRP laminates with 90° ply of different thicknesses (Table 5) indicates that the laminate with the thicker transverse ply fail at lower stress

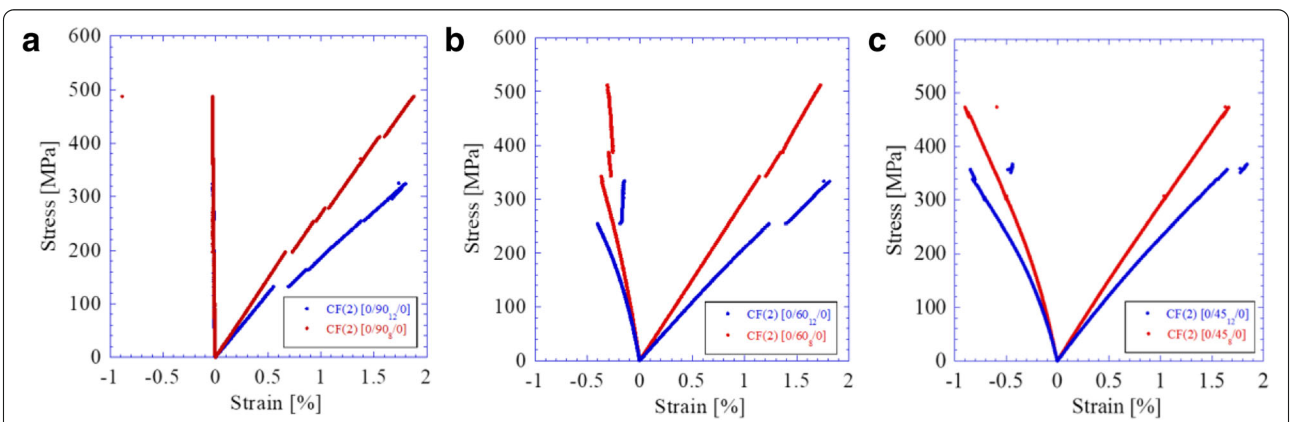

Fig. 4 Strain-stress curve for CFRP[2] laminates with different orientation of the off-axis ply: **a** 90 °, **b** 60 ° and **c** 45°

Table 5 Average mechanical properties of tested CFRP laminates

CFRP	Laminates structure	Young's modulus [GPa]	Tensile strength [MPa]	Max longitudinal strain [%]	Poisson's ratio
[1] (T700SC/2500)	$[0_3/90_{24}/0_3]$	30.4	523	1.96	0.031
	$[0_3/90_{36}/0_3]$	24.2	306	1.60	0.030
	$[0_3/75_{24}/0_3]$	32.9	503	1.74	0.091
	$[0_3/75_{36}/0_3]$	23.7	367	1.94	0.086
	$[0_3/45_{24}/0_3]$	32.0	538	1.83	0.344
	$[0_3/45_{36}/0_3]$	25.5	359	1.60	0.330
[2] (T700SC/2592)	$[0/90_8/0]$	29.3	476	1.81	0.027
	$[0/90_{12}/0]$	24.5	326	1.73	0.030
	$[0/60_8/0]$	29.9	516	1.87	0.218
	$[0/60_{12}/0]$	24.6	360	1.75	0.227
	$[0/45_8/0]$	33.3	542	1.62	0.402
	$[0/45_{12}/0]$	24.8	365	1.76	0.328

than the laminate with the thinner transverse ply. Similar behavior can be observed in the angle-ply laminates where thinner laminates showed higher stiffness and strength, as can be seen in Figs. 3b & c and 4b & c and Table 5. This is because the Energy Release Rate (ERR) associated with the formation of cracks in the thicker laminates is higher, thus caused cracks to form earlier in the thicker laminates.

For laminates with the same number of plies and the off-axis angle decreasing from 90° to 45°, there are no remarkable differences in the Young's modulus. The Poisson's ratio, however, increases significantly as the off-axis angle decreases, as would be expected, since the contribution of the mid-ply matrix to strain in the transverse direction increases. These results for the Young's modulus and Poisson's ratio are in agreement with the Classical Laminate Theory. It can also be observed that variation of the off-axis angle has a marginal effect on the tensile strength of the laminates.

GFRP laminates

Table 6 shows the mechanical properties (average of 3 specimens) of tested GFRP laminates. The corresponding stress-strain curves can be seen in Fig. 5. As expected, the Young's modulus and tensile strength of GFRP laminates are markedly lower than of CFRP laminates due to lower stiffness in fiber direction. On the other hand, the GFRP laminates exhibit the larger fracture longitudinal strain and Poisson's ratio than the CFRP laminates showing more ductility. Similar to the CFRP laminates, the thicker off-axis plies laminates of GFRP also failed at a lower stress than the thinner laminate with the same orientation of the off-axis ply. With the off-axis angle varying from 90° to 60°, the Poisson's ratio increased. The cross-ply $[0_3/90_{24}/0_3]$ specimens showed the same Poisson's ratio and the value of maximum strain at failure as the specimens prepared from the same laminate and rotated by -15°, $[-15_3/75_{24}/-15_3]$.

Loading-unloading tensile test

Nonlinearity in the stress-strain curve obtained from monotonic tensile loading is mainly associated with formation of new cracks in the laminate. Once new cracks have formed, subsequent unloading follows a new linear stress-strain relationship, which reflects the effect of the formed cracks on the properties of the laminate. Therefore, unloading that does not induce additional damage in the laminate allows to observe the effects of damage in a more clear way.

Table 6 Mechanical properties of every GFRP laminates tested

GFRP Laminates	Young's modulus [GPa]	Tensile strength [MPa]	Max longitudinal strain [%]	Poisson's ratio
$[0_3/90_{24}/0_3]$	16.8	211	2.61	0.104
$[0_3/90_{12}/0_3]$	21.0	314	1.90	0.106
$[0_3/75_{24}/0_3]$	16.3	212	2.74	0.150
$[-15_3/75_{24}/-15_3]$	14.2	132	2.61	0.104
$[0_3/60_{24}/0_3]$	15.9	227	2.44	0.307

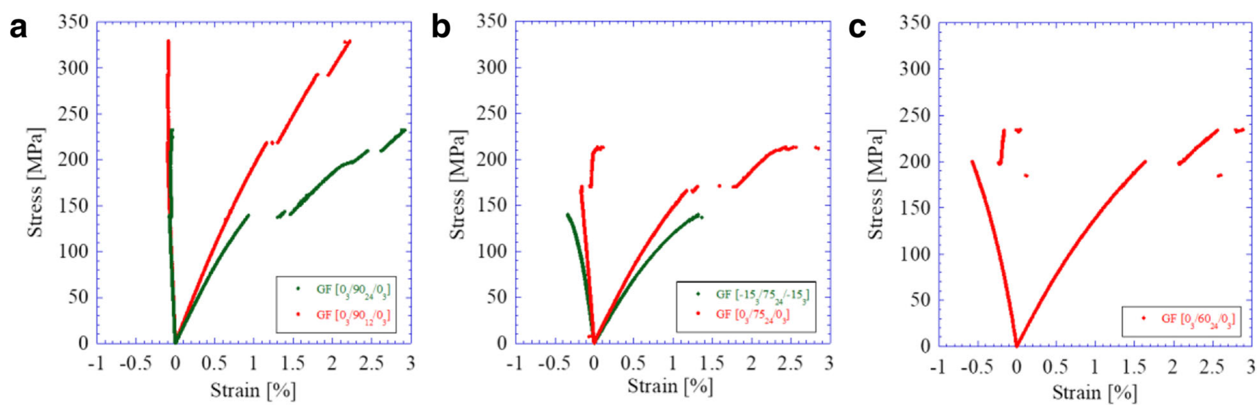

Fig. 5 Strain-stress curve for GFRP laminates with different orientation of the off-axis ply: **a** 90, **b** 75 and **c** 60°

Figures 6, 7, 8, 9, 10 and 11 show the stress-strain curves recorded during cyclic loading. It can be seen that the gradients of stress-strain curve gradually decrease with every cycle due to a decrease in stiffness of the laminates after the formation of the cracks. The stiffness was calculated at strain of 0.1%~ 0.3%, 0.2%~ 0.4% or 0.3~ 0.5% following formation of new cracks at every cycle. The Figures also demonstrate existence and a gradual increase in residual strains as the laminates are unloaded back to zero stress at the end of each loading-unloading cycle. This is related to relief of curing stresses due to formation of intralaminar cracks.

CFRP laminates

Figures 6, 7, 8 and 9 show stress-strain curves obtained from loading-unloading tensile test for CFRP[1] $[0_3/75_{24}/0_3]$, $[0_3/75_{36}/0_3]$ and CFRP[2] $[0/90_8/0]$, $[0/60_8/0]$ laminates. From the result for CFRP[1] $[0_3/75_n/0_3]$ laminates in Figs. 6 and 7, nonlinearity associated with onset of cracking is observed at higher strains in laminates with thinner off-axis plies. Similar results were obtained for the laminate configurations that have off-axis angle of 45°, 60° and 90° for both CFRP[1] and CFRP[2]. This happened also because the ERR associated with the formation of cracks is smaller in thinner laminates. Hence, the cracks started to form later at higher applied strain than in thicker laminates. Laminates with lower off-axis angles, such as 45° or 60 °, started to show nonlinearity at a higher strain (Fig. 9). In laminates of the same thickness the strain of initial nonlinearity increases as

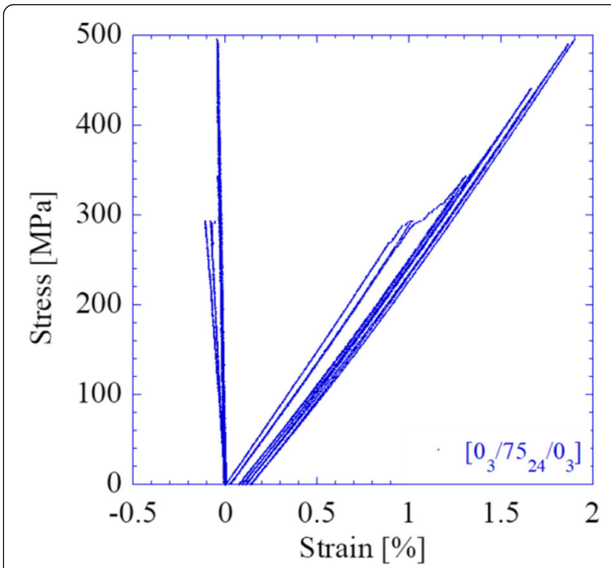

Fig. 6 Stress-strain curve of CFRP[1] $[0_3/75_{24}/0_3]$ laminate for loading-unloading tensile test

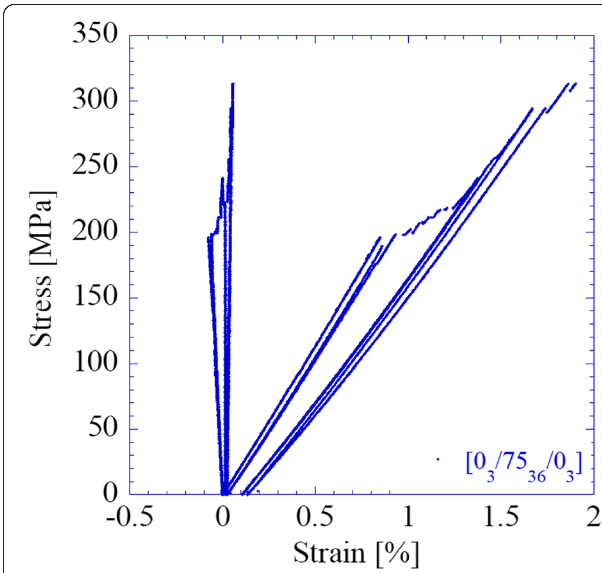

Fig. 7 Stress-strain curve of CFRP[1] $[0_3/75_{36}/0_3]$ laminate for loading-unloading tensile test

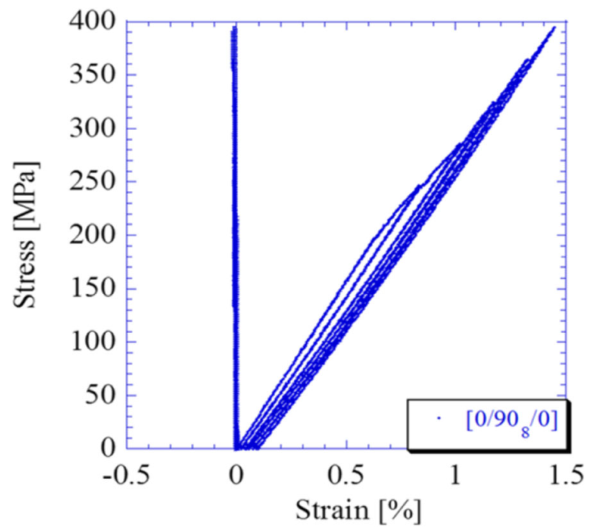

Fig. 8 Stress-strain curve of CFRP[2] [0/90$_8$/0] laminate for loading-unloading tensile test

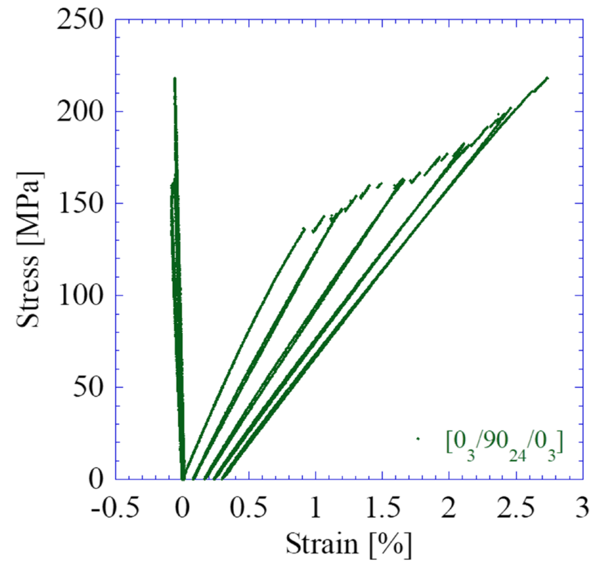

Fig. 10 Stress-strain curve of GFRP [0$_3$/90$_{24}$/0$_3$] laminate for loading-unloading tensile test

the off-axis angle changes from 90^o to 45^o. Therefore, the changes in off-axis angle have a significant effect on the cracking onset strains.

Furthermore, the transverse strains are larger in laminates with off-axis angle 45^o than in laminates with off-axis angle 90^o. As shown in Fig. 8, [0/90$_8$/0] laminate showed very small residual strains in the transverse direction and gradient changes with cycling when compared to [0/60$_8$/0] laminate (Fig. 9). This shows that the residual strain in transverse direction increases with the decreasing off-axis ply angle.

GFRP laminates

Figures 10 and 11 show stress-strain curves obtained from loading-unloading tensile tests carried out with GFRP [0$_3$/90$_{24}$/0$_3$], and [− 15$_3$/75$_{24}$/− 15$_3$] laminates, respectively. Same as in CFRP laminates, for all of the laminates tested, as off-axis angle decreases from 90^o to 60^o, the strain of nonlinearity onset increases. For [0$_3$/90$_{24}$/0$_3$] laminates, Fig. 10, the residual strains in both the laminates in the transverse direction are also very small; the hysteresis loop formed within the range of − 0.1~

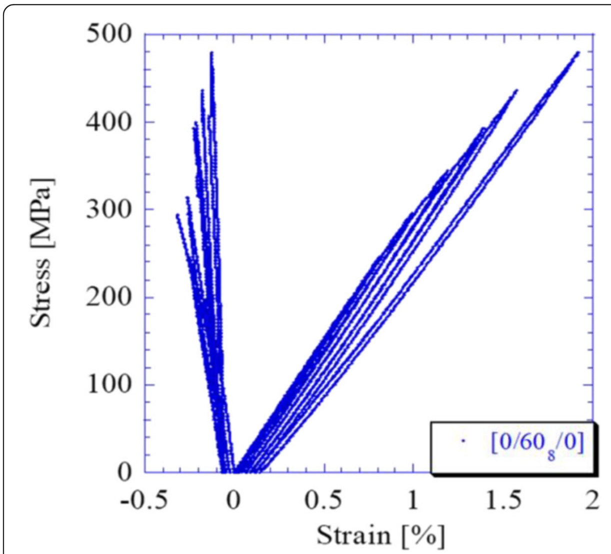

Fig. 9 Stress-strain curve of CFRP[2] [0/60$_8$/0] laminate for loading-unloading tensile test

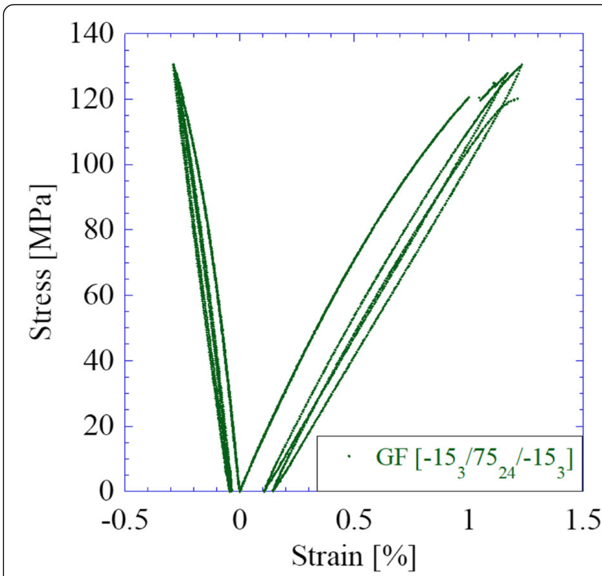

Fig. 11 Stress-strain curve of GFRP [− 15$_3$/75$_{24}$/− 15$_3$] laminate for loading-unloading tensile test

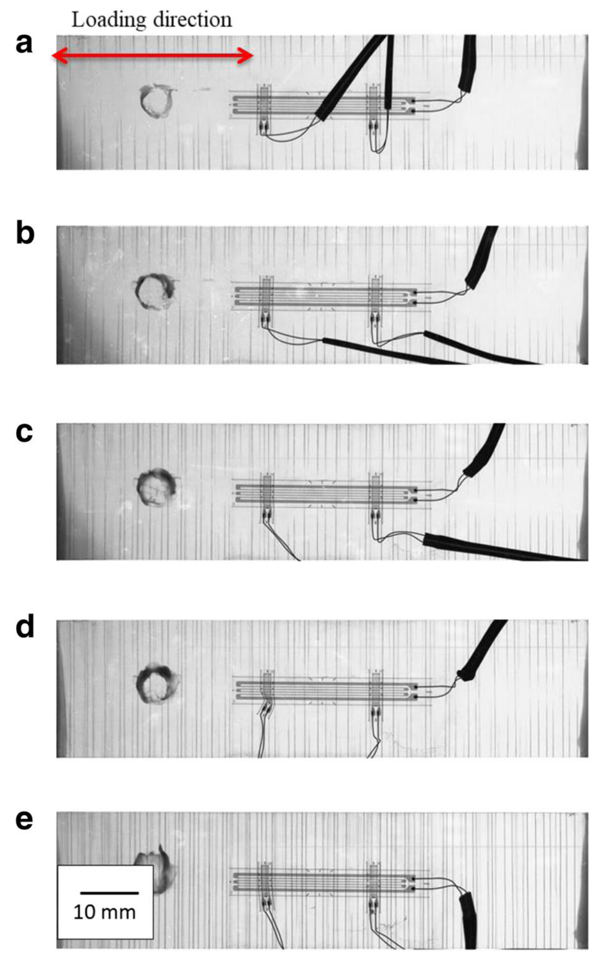

Fig. 12 X-ray images of CFRP[1] $[0_3/90_{24}/0_3]$ laminate **a** $\sigma = 300[MPa]$, $\varepsilon = 1.14[\%]$, **b** $\sigma = 350[MPa]$, $\varepsilon = 1.35[\%]$, **c** $\sigma = 400[MPa]$, $\varepsilon = 1.55[\%]$, **d** $\sigma = 450[MPa]$, $\varepsilon = 1.75[\%]$, (**e**) $\sigma = 500[MPa]$, $\varepsilon = 1.94[\%]$

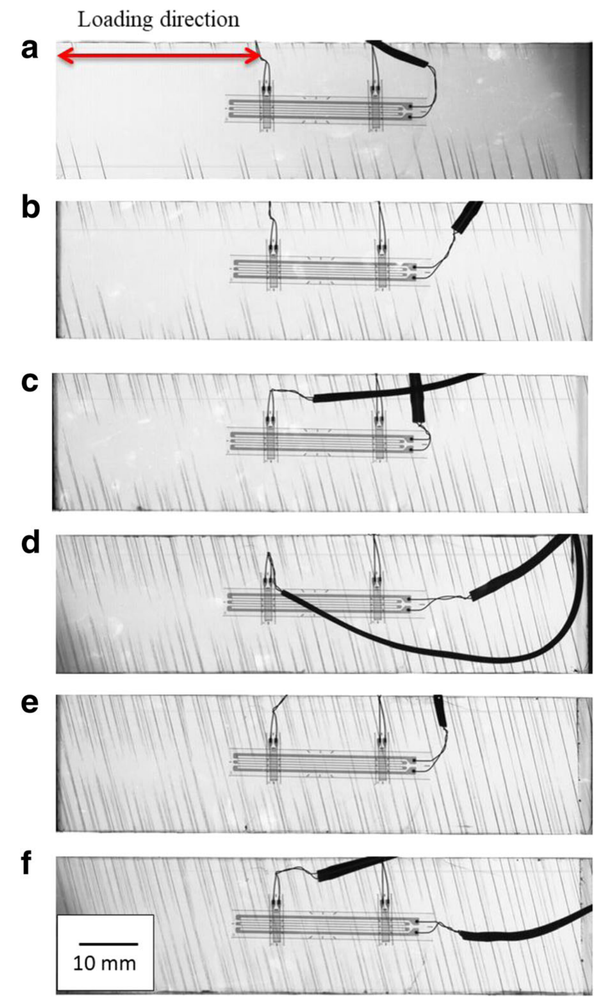

Fig. 13 X-ray images of CFRP[1] $[0_3/75_{24}/0_3]$ laminate **a** $\sigma = 300[MPa]$, $\varepsilon = 1.10[\%]$, **b** $\sigma = 320[MPa]$, $\varepsilon = 1.24[\%]$, **c** $\sigma = 340[MPa]$, $\varepsilon = 1.31[\%]$, **d** $\sigma = 360[MPa]$, $\varepsilon = 1.42[\%]$, **e** $\sigma = 400[MPa]$, $\varepsilon = 1.59[\%]$, **f** $\sigma = 430[MPa]$, $\varepsilon = 1.75[\%]$

0%. The same applies to $[0_3/90_{36}/0_3]$ laminates. As shown in Fig. 11, residual strains in the transverse direction in $[-15_3/75_{24}/-15_3]$ laminate are larger than in $[0_3/90_{24}/0_3]$ laminates and the hysteresis loop can clearly be observed. Furthermore, the cyclic change in the transverse strain increased as well. Rotation of the cross-ply laminate by -15° caused the nonlinear stress-strain behavior to start earlier. Due to the existence of -15° laminate, the laminate fractured by developing delamination cracks at the interfaces between – 15 and 75° plies and matrix cracks in the outer 75° plies.

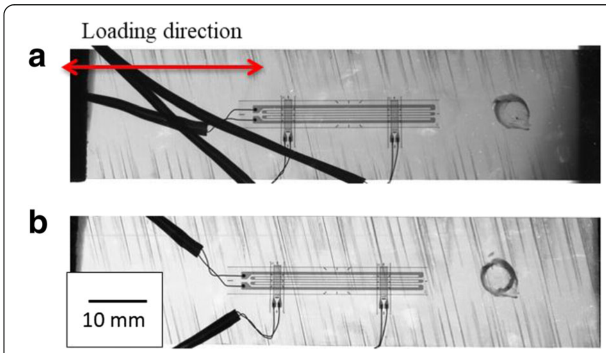

Fig. 14 X-ray images of CFRP[1] $[0_3/75_{36}/0_3]$ laminate **a** $\sigma = 250[MPa]$, $\varepsilon = 1.31[\%]$, **b** $\sigma = 300[MPa]$, $\varepsilon = 1.61[\%]$

Crack observation

For CFRP[2] cross-ply $[0/90_{12}/0]$, $[0/90_8/0]$ and all CFRP[1] laminates, X-ray images were taken after unloading and removing from the tensile test machine, followed by remounting the specimens in the machine.

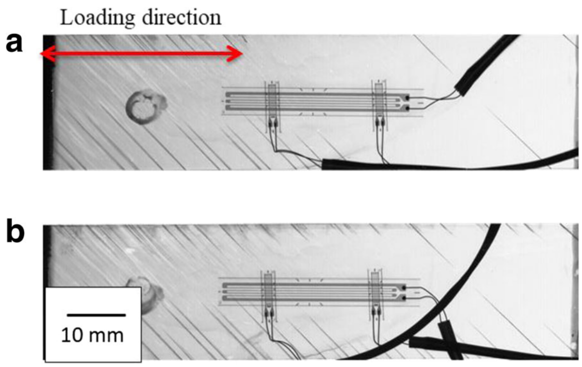

Fig. 15 X-ray images of CFRP[1] $[0_3/45_{36}/0_3]$ laminate **a** $\sigma = 294[MPa]$, $\varepsilon = 1.34[\%]$, **b** $\sigma = 342[MPa]$, $\varepsilon = 1.73[\%]$

For CFRP[2] $[0/60_{12}/0]$, $[0/60_8/0]$, $[0/45_{12}/0]$ and $[0/45_8/0]$ laminates, the X-ray images were taken after the artificial notches were removed. For GFRP laminates, due to its semi-permanent properties, cracks formation can be observed in real-time, tracing the crack density-strain relationship can be investigated. The cracks were observed

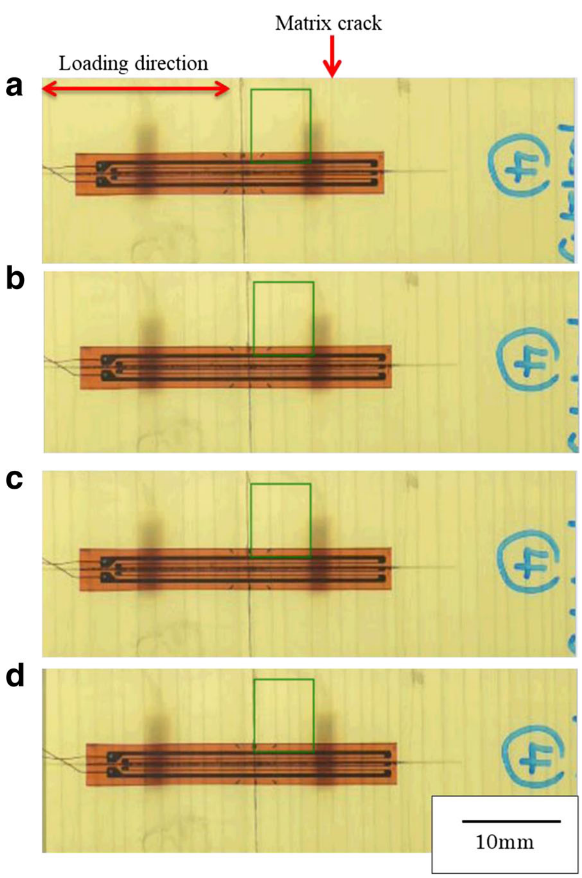

Fig. 16 Images of cracks in GFRP $[0_3/90_{12}/0_3]$ laminate **a** $\sigma = 200[MPa]$, $\varepsilon = 1.15[\%]$, **b** $\sigma = 225[MPa]$, $\varepsilon = 1.50[\%]$, **c** $\sigma = 255[MPa]$, $\varepsilon = 1.73[\%]$, **d** $\sigma = 285[MPa]$, $\varepsilon = 2.02[\%]$

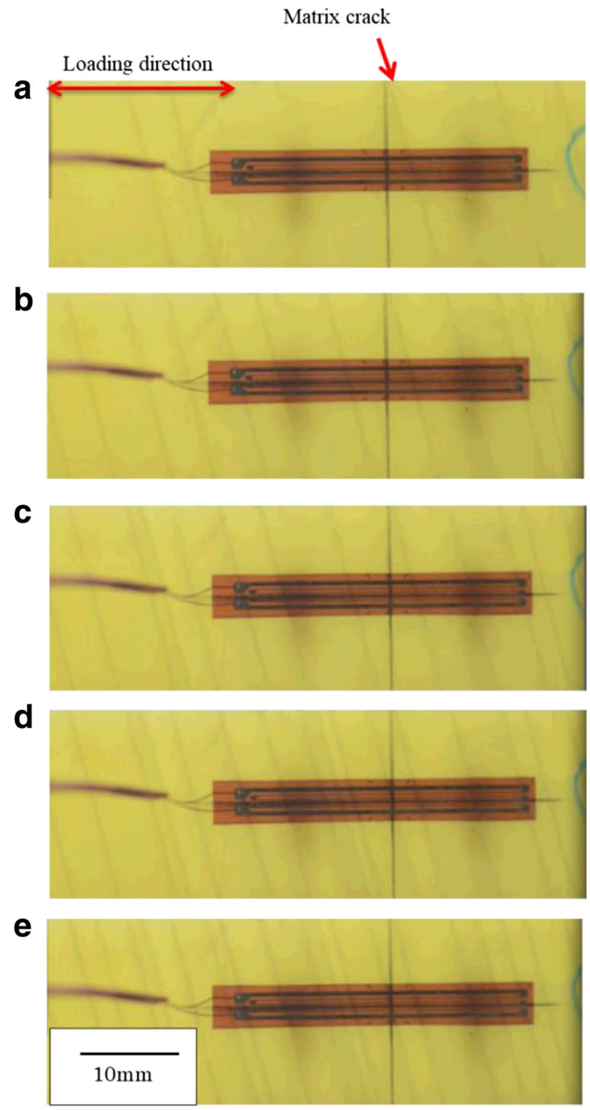

Fig. 17 Images of cracks in GFRP $[0_3/75_{24}/0_3]$ laminate **a** $\sigma = 160[MPa]$, $\varepsilon = 1.47[\%]$, **b** $\sigma = 170[MPa]$, $\varepsilon = 1.59[\%]$, **c** $\sigma = 180[MPa]$, $\varepsilon = 1.85[\%]$, **d** $\sigma = 190[MPa]$, $\varepsilon = 2.13[\%]$, **e** $\sigma = 200[MPa]$, $\varepsilon = 2.36[\%]$

and counted at specific area on the specimen which is along the length of strain gauge.

CFRP laminates

Figures 12, 13, 14 and 15 show X-ray images of CFRP [1] ($[0_3/90_{24}/0_3]$, $[0_3/75_{24}/0_3]$, $[0_3/75_{36}/0_3]$, and $[0_3/45_{36}/0_3]$) laminates after a loading-unloading tensile test. Initially at lower stress and strain, all results showed that most of the cracks were formed at the edges of the laminates without penetrating through the width of the coupons. As the applied strain increases, more tunneling cracks propagate through to the other edge of the coupon.

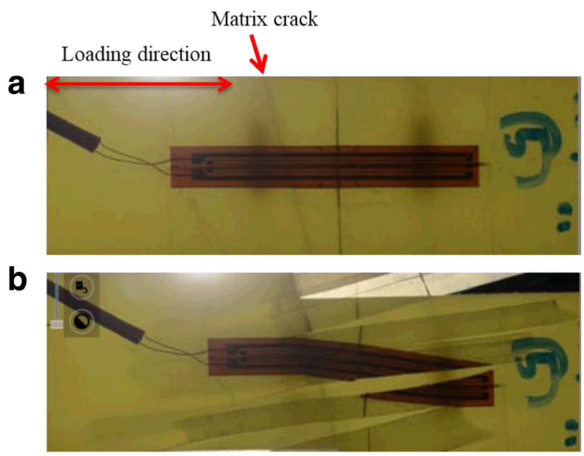

Fig. 18 Images of cracks in GFRP [$-15_3/75_{24}/-15_3$] laminate **a** σ = 130[*MPa*], ε = 1.17[%], **b** σ = *fractured*, ε = 1.21[%]

Laminates with off-axis ply angles of 90° and 75° were loaded 50 MPa above the stress, at which nonlinearity onset in the stress-strain curves was recorded, and unloaded afterwards. As shown in Fig. 12, in CFRP [$0_3/90_{24}/0_3$] laminate at maximum strain of 1.14%, cracks were formed at the coupon edges without extending to the opposite edge. As the applied strain increased to 1.35%, cracks started to penetrate through the entire width of the specimen. Similar observations were obtained for the other layups.

Comparison of crack formation in laminates of different thicknesses indicates that crack initiation at the coupon edges occur at lower strains in thicker laminates. Both crack propagation in the width direction and the rate of new crack formation is slower in the thicker laminates, as can be seen in the X-Ray images of Figs. 13 and 14 performed for [$0_3/75_{36}/0_3$] and [$0_3/75_{24}/0_3$] laminates. A possible reason for this phenomenon is also because the ERR associated with the cracks occurrence in the laminate become bigger as the middle ply becomes thicker. This causes the cracks to form at lower stress and strain and decreases the rate of new crack formation in the thicker laminates. For laminates with different off-axis ply angle, decrease from 90° to 45° makes crack formation more effort demanding. For example, in Fig. 15, none of the edge cracks propagated entirely through the coupon width. Similar results were obtained for CFRP [2] laminates.

GFRP laminates

In contrast to the cracking processes in CFRP laminates described above, cracks in GFRP laminates crossed the entire width of the laminate instantaneously. Cracks in GFRP laminates also formed at a lower stress and strain compared to CFRP laminates. Since GFRP laminates are transparent, new crack formation can be observed in-situ, while recording the corresponding values of applied strain.

Figure 16 shows snapshots of a cross-ply coupon at different stress/strain levels, demonstrating increasing crack density with the applied strain. Figures 17 and 18 show images of GFRP [$0_3/75_{24}/0_3$] and [$-15_3/75_{24}/-15_3$] angle-ply laminates with corresponding values of applied stress and strain. For [$-15_3/75_{24}/-15_3$] laminate, only one crack was observed within the inspection zone before failure at 1.21% strain, when the laminate fractured by forming cracks in the outer plies and delamination cracks between – 15 ° and 75° plies. The laminate with layup [$0_3/75_{24}/0_3$], on the other hand, showed gradually increasing crack density with increasing applies strain. Comparison of all laminate configurations indicates that fewer cracks form in laminates with smaller angles of the off-axis plies at the same applied strain.

Artificial cracks observation

Figures 19 and 20 show the X-ray images of CFRP[2] [$0/60_8/0$] and [$0/60_{12}/0$] laminates, respectively. The cracks in these laminates originated from artificial notches made at the free edges of the laminates. Not all of the multiple notches propagated across the specimens, possibly because the notches were made manually with inconstant force and angles. Less cracks formed from the

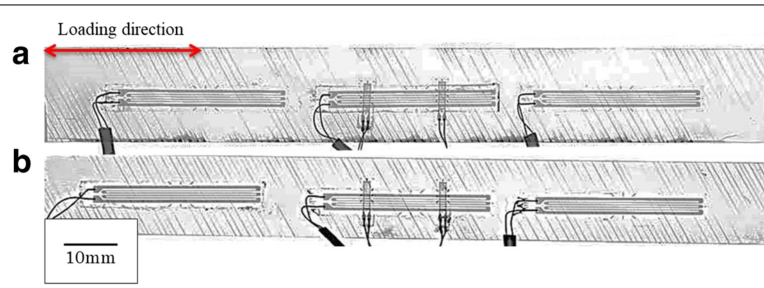

Fig. 19 X-ray images of CFRP[2] [$0/60_8/0$] laminate **a** 1st specimen **b** 2nd specimen

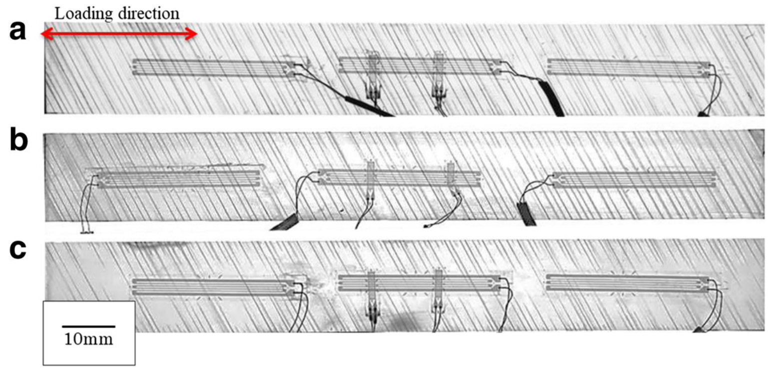

Fig. 20 X-ray images of CFRP[2] $[0/60_{12}/0]$ laminate **a** 1st specimen **b** 2nd specimen **c** 3rd specimen

notches in the thinner $[0/60_8/0]$ laminate than in $[0/60_{12}/0]$. Even fewer cracks formed in laminates with a lower off-axis angle of 45°, which partially can be attributed to inconsistency in the notch directions, and notches not being aligned with the fiber direction, consequently leading to lower stress intensity than in the case of 60° plies. The X-ray observations were done on the specimens after the artificial notches had been removed, so that the result for the stiffness reduction and crack density relationship were not affected by the notches on the edges of the specimens.

Stiffness reduction due to matrix cracking and comparison to variational analysis

Stiffness reduction is typically presented by normalizing the stiffness of the cracked laminate by the stiffness of the virgin laminate. Crack density can be defined as the total length of cracks propagated in the off-axis ply direction within the observation area divided by the area, or alternatively, the crack density is reciprocal of the average (shortest) distance between adjacent cracks. The laminate stiffness reduction is a good indicator of the damage state in the material, if for a particular laminate system a unique relationship between the damage (crack density) and the stiffness reduction is known.

Figures 21, 22 and 23 show the results for stiffness reduction vs crack density obtained experimentally and analytically for CFRP[1], CFRP[2] and GFRP laminates. The experimental data represents results for two or more laminate specimens tested in loading-unloading, as well as those with artificially induced cracks. The analytical curves represent the results of a variational analysis. The method is based on building an admissible stress field in a fragment of a cracked laminate that satisfies the equilibrium conditions, continuity of tractions at the interfaces and zero traction at the open crack surfaces. It assumes a certain through the thickness dependency of the in-plane stresses, while the dependency in the direction perpendicular to the existing intralaminar cracks is obtained from the complimentary energy minimization. For the layups in the present experimental study, the variational analysis of Vinogradov and Hashin (2010) is the most suitable, as it considers laminates of the type $[\theta_m/\phi_n]_s$. However, following the original assumptions of Hashin (1986), the method assumes a piece-wise constant distribution of stresses in the thickness direction, which for some, especially thick laminates, tends to underestimate the Young's modulus, when compared to the experimental data presented here. The more general variational approach of Vinogradov (2015), which is used herein, assumes a linear stress distribution in the thickness direction and allows ply refinement, when plies can be subdivided into several sub-plies, leading to a more accurate description of the stress field, and consequently, a better estimate for the effective Young's modulus.

As can be seen in Figs. 21, 22 and 23, for all laminate layups and materials, the differences in stiffness reduction of the thin and thick laminates can be seen quite distinctively, when higher stiffness reduction is observed in the thicker laminates with the same off-axis ply orientation. At the same time, laminates with 0^o outer ply and the same thickness show a marginal effect of the middle ply orientation on the normalized Young's modulus, e.g., compare laminates with 24 mid-ply laminae and different orientations (upper curves) in Figs. 21a-c or 8-laminae layups in Fig. 22. In Fig. 22a experimental data for an additional CFRP[2] laminate with layup $[-15/75_{12}/-15]$ is also included. It can be seen that rotation of the cross-ply $[0/90_{12}/0]$ by 15^o leads to dramatic differences in the normalized stiffness reduction rates. Much smaller differences are predicted analytically for rotation of GFRP $[0_3/90_{24}/0_3]$ by -15^o to form $[-15_3/75_{24}/-15_3]$, as shown in Fig. 23a, b, however, as described above, this laminate failed after just one crack has formed within the observation zone (Fig. 18).

In view of the fact that the variational analysis provides the lower bound for stiffness reduction and crack density relation, the analytical and experimental results for the

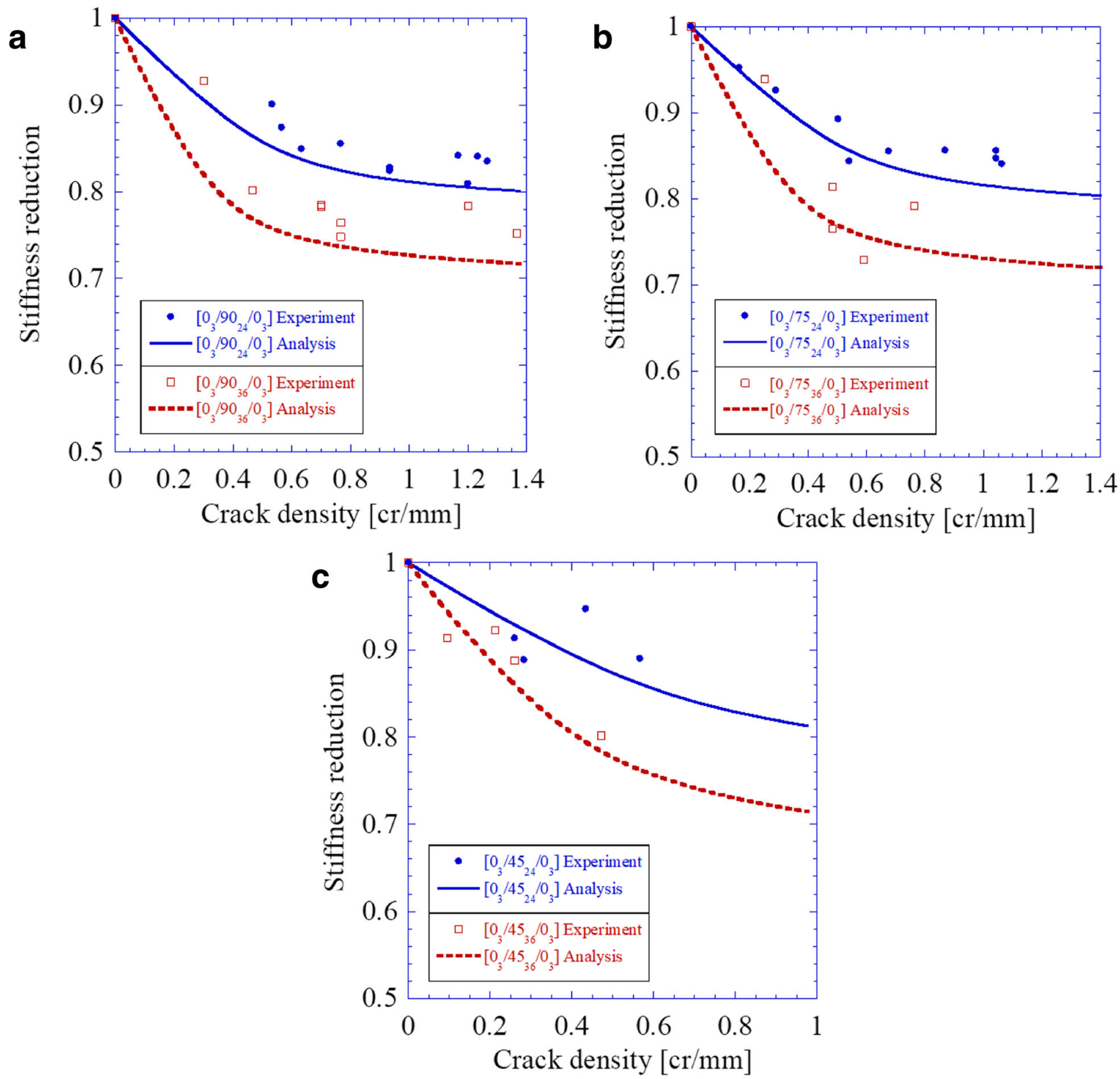

Fig. 21 a Off-axis angle: 90°, **b** 75°, **c** 45°)

studied laminates are in good agreement, as most of the experimental data points stay on or slightly above the analytical curves. However, there are several ocasions where experimental data are lower than the analytical prediction. Possible reasons for this could be variation in the secimen properties and formation of uncounted cracks close to, but outside the observation zone, and could effect the results. Some dispersion in the experimental data could also be caused by randomness in the mechanical properties of the material, effects of the notches at the edges of the specimen on the 0° outer ply. In addition, the CFRP [1] laminates showed multiple small cracks occurred at the free edges which did not penetrate along the specimen, which could affect the stiffness reduction measurements as well.

Conclusion

Intralaminar damage behavior and its effects on the mechanical properties of several angle-ply FRP laminates were investigated. CFRP and GFRP laminates with fiber configuration of $[\,\theta_{\mathrm{m}}\,/\,\sigma_n\,]_{\mathrm{s}}$ were used in this study. In order to study the damage behavior and its effects, the laminates were loaded monotonically and cyclically and cracks observations were carried out. In

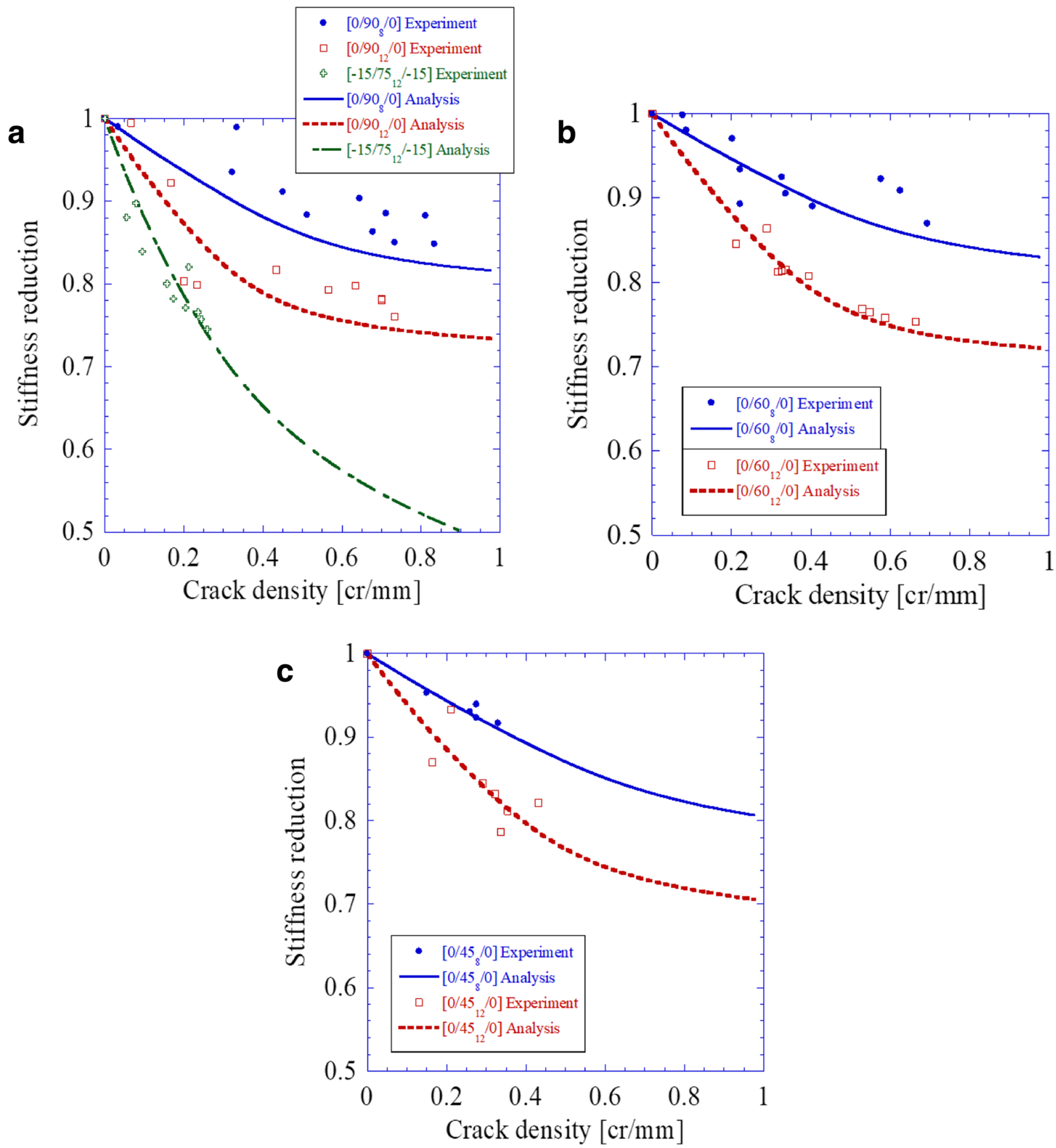

Fig. 22 a Off-axis angle: 90° and 75°, **b** 60°, **c** 45°

some angle-ply laminates, artificial cracks method were used before the laminates were monotonically loaded, so that higher crack densities could be attained. From monotonic tensile tests, it can be understood that as the middle off-axis ply becomes thicker, the Young's modulus and maximum tensile stress of the laminates decreases. On the other hand, the differences in off-axis orientations have marginal effects on the stiffness and strength of a laminate. From the cyclic loading results, for CFRP laminates of the same thickness, changes in the off-axis angle from 90° to 45°, earlier cracking initiation and observed nonlinearity of the stress-strain curves were recorded. Changes in the transverse strain, which

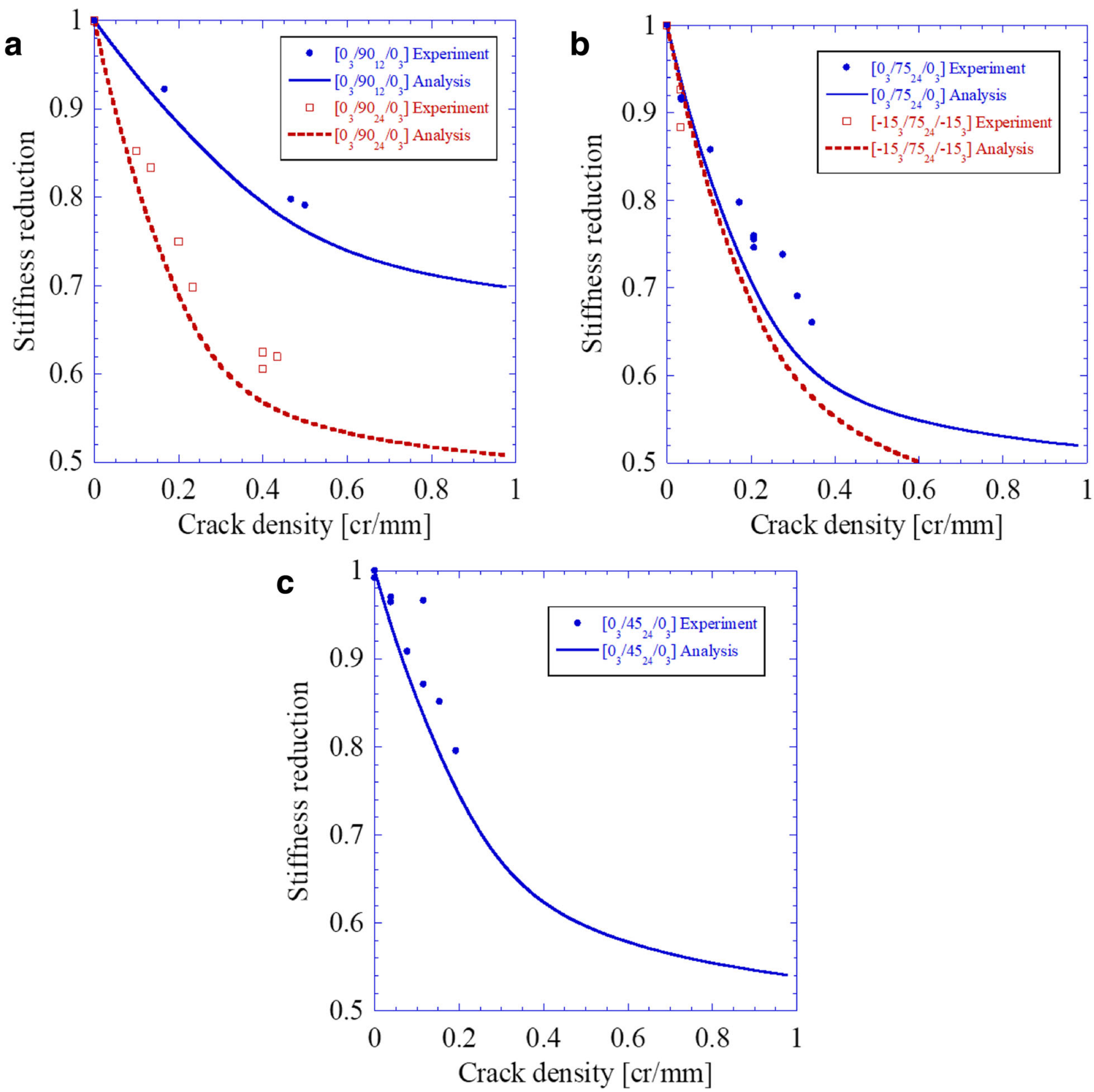

Fig. 23 a Off-axis angle: 90°, **b** 75°, **c** 45°

reflect the effective Poisson's ratio of the laminate, were larger in laminates with off-axis angle 45° than in laminates with off-axis angle 90°. For CFRP laminates, it can be observed that first cracks mostly formed and accumulated at free edges. Crack propagation rates in the width direction were dependent on the thickness of the middle ply. In contrast to CFRP laminates, cracks in GFRP laminates formed instantaneously propagating in the width direction. Stiffness in laminates with the thicker off-axis plies reduced more. The experimental data and predictions of the variational analysis are found in good agreement for the Young's modulus of the cracked laminate. Based on these results, we hope that in future work, we can study laminates of higher practical imprtance. The comparison of both experimental result and analytical result demonstrated the ability of the approaches to accurately predict the effect of transverse cracking on the stiffness of the laminates, independently on their layups. Systematic analysis of residual strains due to increasing crack density will be addressed in future publications.

Acknowledgments
Special thanks of gratitude to MARA Education Foundation (YPM) for sponsoring the corresponding author to study in Japan in order to complete this research study.

Availability of data and materials
Please contact author for data requests.

Authors' contributions
MF carried out the experimental studies, participated in the sequence alignment and drafted the manuscript. VV participated in the design of the study and performed the variational analysis. SO conceived of the study, and participated in its design and coordination and helped to draft the manuscript. All authors read and approved the final manuscript.

Competing interests
The authors declare that they have no competing interests.

Publisher's Note
Springer Nature remains neutral with regard to jurisdictional claims in published maps and institutional affiliations.

Author details
[1]Department of Mechanical Engineering, Graduate School of Science and Technology, Tokyo, University of Science, 2641 Yamazaki, Noda-shi, Chiba-ken, Japan. [2]Department of Mechanical Engineering, Faculty of Science and Technology, Tokyo University of Science, 2641 Yamazaki, Noda-shi, Chiba-ken, Japan. [3]School of Engineering, Newcastle University, Newcastle upon Tyne NE1 7RU, UK.

Received: 23 March 2018 Accepted: 24 July 2018
Published online: 04 August 2018

References
Bassam F, Boniface L, Jones K, Ogin SL (1998) On the behaviour of the residual strain produced by matrix cracking in cross-ply laminates. Compos A: Appl Sci Manuf 29:1425–1432
Harrison RP, Bader MG (1983) Damage development in CFRP laminates under monotonic and cyclic stressing. Fibre Sci Technol 18(3):163–180
Hashin Z (1985) Analysis of cracked laminates. Mech Mater 4(2):121–136
Hashin Z (1986) Analysis of stiffness reduction of cracked cross-ply laminates. Eng Fract Mech 25(5–6):771–778
Hashin Z (1988) Thermal expansion coefficients of cracked laminates. Compos Sci Technol 31(4):247–260
Highsmith AL, Reifsnider KL (1982) Stiffness-Reduction Mechanisms in Composite Laminates. Damage in Composite Materials, ASTM STP 775. American Society for Testing and Materials, Philadelphia, pp 103–117
Jones RM (1975) Mechanics of composite materials. Scripta Book Company, Washington, DC
Katerelos DG, McCartney LN, Galiotis C (2006) Effect of off – Axis matrix cracking on stiffness of symmetric angle-ply composite laminates. Int J Fract 139:529–536
Katerelos DTG, Krasnikovs A, Varna J (2015) Variational models for shear modulus of symmetric and balanced laminates with cracks in 90-layer. Int J Solids Struct 71:169–179
Li S, Hafeez F (2009) Variation-based cracked laminate analysis revisited and fundamentally extended. Int J Solids Struct 46:3505–3515
Nairn JA (1992) Microcraking, microcrack-induced delamination, and longitudinal splitting of advance composite structures. NASA Contractor Rep 4472:5–71
Nairn JA, Shoufeng HU (1992) The formation and effect of outer-ply microcracks in cross-ply laminates: a Variational approach. Eng Fract Mech 41(2):203–221
Nouri H, Lubineau G, Traudes D (2013) An experimental investigation of the effect of shear-induced diffuse damage on transverse cracking in carbon-fiber reinforced laminates. Composite Struct 106:529–536
Singh CV (2008) Analysis of multiple off-axis ply cracks in composite laminates. Int J Solids Struct 45(16):4574–4589
Tong J et al. (1997) On matrix crack growth in quasi-isotropic laminates—II. Finite element analysis. Composites Sci Technol 57(11):1537–1545
Vinogradov V 2015 Analysis of initial accumulation of matrix cracks in angle-ply laminates. In: Proceedings of 20th International Conference on Composite Materials (ICCM20). 2015. Copenhagen, Denmark.
Vinogradov V, Hashin Z (2010) Variational analysis of cracked angle-ply laminates. Compos Sci Technol 70(4):638–646